Yariv, *Phys. Rev. Lett.* **73**, 3211 (1994); D. N. Christodoulides and M. I. Carvalho, *J. Opt. Soc. Am. B* **12**, 1628, (1995); M. Segev, M. Shih, G. C. Valley, *J. Opt. Soc. Am. B* **13**, 706 (1996).
22. M. D. Iturbe-Castillo, P. A. Marquez-Aguilar, J. J. Sanchez-Mondragon, S. Stepanov, V. Vysloukh, *Appl. Phys. Lett.* **64**, 408 (1994).
23. M. Shih *et al.*, *Electron. Lett.* **31**, 826 (1995); *Opt. Lett.* **21**, 324 (1996).
24. D. Kip, M. Wesner, V. Shandarov, P. Moretti, *Opt. Lett.* **23**, 921 (1998).
25. Y. N. Karamzin and A. P. Sukhorukov, *Sov. Phys. JETP* **41**, 414 (1976).
26. W. E. Torruellas *et al.*, *Phys. Rev. Lett.* **74**, 5036 (1995); R. Schiek, Y. Baek, G. I. Stegeman, *Phys. Rev. E* **53**, 1138, (1996).
27. R. A. Fuerst, M. T. G. Canva, D. Baboiu, G. I. Stegeman, *Opt. Lett.* **22**, 1748 (1997); P. Di Trapani, G. Valiulis, W. Chinaglia, A. Adreoni, *Phys. Rev. Lett.* **80**, 265 (1998).
28. All nonlinearities are actually noninstantaneous, because even in the fastest nonlinear medium possible the shortest response time is the dephasing time (or the life-time, for real energy levels).
29. M. Mitchell, Z. Chen, M. Shih, M. Segev, *Phys. Rev. Lett.* **77**, 490 (1996); Z. Chen, M. Mitchell, M. Segev, T. H. Coskun, D. N. Christodoulides, *Science* **280**, 889 (1998).
30. M. Mitchell and M. Segev, *Nature* **387**, 880 (1997).
31. Strictly speaking, quadratic solitons can be thought of as composite solitons because they involve mutual self-trapping of two (or more) optical fields.
32. When the jointly induced waveguide has a stationary shape, the propagating fields can have oscillating (nonstationary) intensities, as long as the total intensity does not change throughout propagation.
33. S. V. Manakov, *Sov. Phys. JETP* **38**, 248 (1974).
34. The term "vector solitons" stands for solitons consisting of two or more components, which includes the case in which the components are orthogonally polarized.
35. J. U. Kang, G. I. Stegeman, J. S. Aitchison, N. Akhmediev, *Phys. Rev. Lett.* **76**, 3699 (1996).
36. S. Trillo, S. Wabnitz, E. M. Wright, G. I. Stegeman, *Opt. Lett.* **13**, 871 (1988).
37. M. Shalaby and A. J. Barthelemy, *IEEE J. Quantum Electron.* **28**, 2736 (1992).
38. D. N. Christodoulides, S. R. Singh, M. I. Carvalho, M. Segev, *Appl. Phys. Lett.* **68**, 1763 (1996); Z. Chen, M. Segev, T. Coskun, D. N. Christodoulides, *Opt. Lett.* **21**, 1436 (1996).
39. D. N. Christodoulides and R. I. Joseph, *Opt. Lett.* **13**, 53 (1988); M. V. Tratnik and J. E. Sipe, *Phys. Rev. A* **38**, 2001 (1988); M. Haelterman, A. P. Sheppard, A. W. Snyder, *Opt. Lett.* **18**, 1406 (1993).
40. A. W. Snyder, S. J. Hewlett, D. J. Mitchell, *Phys. Rev. Lett.* **72**, 1012 (1994).
41. M. Mitchell, M. Segev, D. N. Christodoulides, *Phys. Rev. Lett.* **80**, 4657 (1998).
42. E. A. Ostrovskaya, Y. S. Kivshar, D. V. Skryabin, W. J. Firth, *Phys. Rev. Lett.* **83**, 296 (1999).
43. D. N. Christodoulides, *Phys. Lett. A* **132**, 451 (1988).
44. Z. Chen *et al.*, *Opt. Lett.* **21**, 1821 (1996).
45. J. P. Gordon, *Opt. Lett.* **8**, 596 (1983).
46. D. Andersen and M. Lisak, *Phys. Rev. A* **32**, 2270 (1995).
47. V. E. Zakharov and A. B. Shabat, *Sov. Phys. JETP* **34**, 62 (1972).
48. N. J. Zabusky and M. D. Kruskal, *Phys. Rev. Lett.* **15**, 240 (1965).
49. S. Gatz and J. Herrmann, *IEEE J. Quantum Electron.* **28**, 1732 (1992).
50. A. W. Snyder and A. P. Sheppard, *Opt. Lett.* **18**, 482 (1993).
51. D. M. Baboiu, G. I. Stegeman, L. Torner, *Opt. Lett.* **20**, 2282 (1995); C. Etrich, U. Peschel, F. Lederer, B. Malomed, *Phys. Rev. A* **52**, R3444 (1995); C. Baslev Clausen, P. L. Christiansen, L. Torner, *Opt. Commun.* **136**, 185 (1997); G. Leo and G. Assanto, *J. Opt. Soc. Am. B* **14**, 3151 (1997).
52. M. Shalaby, F. Reynaud, A. Barthelemy, *Opt. Lett.* **17**, 778 (1992).
53. J. S. Aitchison *et al.*, *Opt. Lett.* **16**, 15 (1991); *J. Opt. Soc. Am. B* **8**, 1290 (1991).
54. J. U. Kang, G. I. Stegeman, J. S. Aitchison, *Opt. Lett.*, **21**, 189 (1996).
55. Y. Baek, R. Schiek, G. I. Stegeman, W. Sohler, *Opt. Lett.* **22**, 1550 (1997); B. Constantini, C. De Angelis, A. Barthelemy, B. Bourliaguest, V. Kermene, *Opt. Lett.* **23**, 424 (1998).
56. V. Tikhonenko, J. Christou, B. Luther-Davies, *Phys. Rev. Lett.* **76**, 2698 (1996); *J. Opt. Soc. Am.* **12**, 2046 (1995); here, the solitons were generated from the breakup of a vortex beam in a saturable self-focusing medium. See also W. J. Firth and D. V. Skryabin, *Phys. Rev. Lett.* **79**, 2450 (1997).
57. W. Krolikowski and S. A. Holmstrom, *Opt. Lett.* **22**, 369 (1997).
58. H. Meng, G. Salamo, M. Shih, M. Segev, *Opt. Lett.* **22**, 448 (1997).
59. L. Torner, J. P. Torres, C. R. Menyuk, *Opt. Lett.* **21**, 462 (1996).
60. W. Krolikowski, B. Luther-Davies, C. Denz, T. Tschudi, *Opt. Lett.* **23**, 97 (1998).
61. M. Shih and M. Segev, *Opt. Lett.* **21**, 1538 (1996); M. Shih, Z. Chen, M. Segev, T. Coskun, D. N. Christodoulides, *Appl. Phys. Lett.* **69**, 4151 (1996).
62. M. Shih, M. Segev, G. Salamo, *Phys. Rev. Lett.* **78**, 2551 (1997).
63. A. Buryak, Y. S. Kivshar, M. Shih, M. Segev, *Phys. Rev. Lett.* **82**, 81 (1999).
64. A. Stepken, F. Kaiser, M. R. Belic, W. Krolikowski, *Phys. Rev. E* **58**, R4112 (1998); M. R. Belic, A. Stepken, F. Kaiser, *Phys. Rev. Lett.* **82**, 544 (1999); A. Stepken, M. R. Belic, F. Kaiser, W. Krolikowski, B. Luther-Davies, *Phys. Rev. Lett.* **82**, 540 (1999).
65. D. J. Mitchell, A. W. Snyder, L. Poladian, *Opt. Commun.* **85**, 59 (1991).
66. D. V. Petrov *et al.*, *Opt. Lett.* **23**, 1444 (1998); L. Torner and D. V. Petrov, *Electron. Lett.* **33**, 608 (1997); *J. Opt. Soc. Am.* B **14**, 2017 (1997). The quadratic solitons here evolved from the breakup of a vortex beam and escaped away from each other.
67. V. V. Steblina, Y. S. Kivshar, A. V. Buryak, *Opt. Lett.* **23**, 156 (1998).
68. N. Akhmediev, W. Krolikowski, A. W. Snyder, *Phys. Rev. Lett.* **81**, 4632 (1998); W. Krolikowski, N. Akhmediev, B. Luther-Davies, *Phys. Rev. E* **59**, 4654 (1999).
69. C. Anastassiou *et al.*, *Phys. Rev. Lett.* **83**, 2332 (1999).
70. R. Radhakrishnan, M. Lakshmanan, J. Hietarinta, *Phys. Rev. E* **56**, 2213 (1997); M. H. Jakubowski, K. Steiglitz, R. Squier, *Phys. Rev. E* **58**, 6752 (1998).
71. E. A. Ostrovskaya, Y. S. Kivshar, Z. Chen, M. Segev, *Opt. Lett.* **24**, 327 (1999).
72. Z. H. Musslimani, M. Segev, D. N. Christodoulides, *Opt. Lett.*, in press.
73. A. P. Sheppard and M. Haelterman, *Opt. Lett.* **19**, 859 (1994).
74. This research was supported at Princeton by the U.S. Army Research Office and the National Science Foundation, at the Technion by the Israel Science Foundation and by the Israeli Ministry of Science, and at CREOL by the National Science Foundation.

REVIEW

Nonlinear Optics for High-Speed Digital Information Processing

D. Cotter,[1]* R. J. Manning,[1] K. J. Blow,[2] A. D. Ellis,[1] A. E. Kelly,[1] D. Nesset,[1] I. D. Phillips,[1] A. J. Poustie,[1] D. C. Rogers[1]

Recent advances in developing nonlinear optical techniques for processing serial digital information at high speed are reviewed. The field has been transformed by the advent of semiconductor nonlinear devices capable of operation at 100 gigabits per second and higher, well beyond the current speed limits of commercial electronics. These devices are expected to become important in future high-capacity communications networks by allowing digital regeneration and other processing functions to be performed on data signals "on the fly" in the optical domain.

Nonlinear optical effects are not part of our everyday experience. At the relatively low light intensities that normally occur in nature, the optical properties of materials at any instant in time are independent of the intensity of illumination. When light waves pass through a medium, there is no interaction between the waves. These are the properties of matter that are familiar to us through our visual sense. However, if the illumination is made sufficiently intense, the optical properties of the medium begin to depend on the intensity and other characteristics of the light. For example, the refractive index n of the medium is changed by an amount $\Delta n = n_2 I$, where I is the optical intensity and n_2 is the nonlinear refraction coefficient. The incident light waves may then interact with each other as well as with the medium. This is the realm of nonlinear optics (*1*, *2*).

Within the past decade, optical fiber cable has been installed in vast quantities in telecommunications networks throughout the world, and the use of light for transmission of information has become ubiquitous. Already,

[1]BT Advanced Communications Technology Centre, Adastral Park, Martlesham Heath, Ipswich IP5 3RE, United Kingdom. [2]Electronic Engineering, Aston University, Aston Triangle, Birmingham, B4 7ET, United Kingdom.

*To whom correspondence should be addressed. E-mail: david.cotter@bt.com

nonlinear optical effects influence the design and performance of advanced high-capacity systems. The optical intensities necessary for telecommunications are often sufficient for nonlinear effects to occur readily in fiber, and these effects have been studied extensively (*3*). Indeed, nonlinear effects are among the dominant factors in determining the range and information carrying capacity of fiber transmission systems (*4*). Here we review recent advances in developing nonlinear optical techniques for processing digital information at high speed in the optical domain.

Digital optical techniques are expected to become increasingly important in future ultra-high-capacity communications networks. Optical transmission systems with capacities of hundreds of gigabits per second are available commercially today, and experimental systems with capacities of several terabits per second on a single fiber have been demonstrated in the laboratory (*5*). These high capacities are achieved by using wavelength division multiplexing to carry many optical channels simultaneously on the same fiber. Single-channel bit rates have also steadily increased with time, both commercially and in research laboratories, and transmission speeds approaching 1 Tbit/s have been demonstrated (*6*). For data rates higher than about 40 Gbit/s, experimental transmission systems often involve the use of nonlinear optical devices to access the data as direct electronic detection is limited in speed. Typically, a nonlinear device is used to demultiplex a lower bit-rate channel, suitable for electronic detection and processing, from a high-speed optical time division multiplexed data stream (Fig. 1A). Blow *et al.* (*7*) demonstrated the potential of nonlinear optical interferometers for this application, with recently reported extensions to very high speed by demultiplexing 10 Gbit/s from 640 Gbit/s (*6*). Another key application of nonlinear optical devices in advanced communication systems is to perform regeneration of signals in the optical domain (Fig. 1B). To overcome the effects of noise, dispersion, crosstalk, and other physical impairments during transmission, full digital regeneration is needed. This so-called 3R regeneration causes the signals to be reamplified, reshaped, and retimed (*8, 9*).

The introduction of these and other digital optical techniques will enable the future development of high-capacity digital photonic networks. Today's networks typically consist of electronic boxes (switches and routers) interconnected by pipes (point-to-point optical transmission systems). Although each pipe can provide huge capacity (several terabits per second), the current boxes-and-pipes network architecture has certain limitations: the electronic box connected at the end of each pipe must be powerful enough to process all the incoming traffic. This is inefficient because a large proportion of this traffic may be in transit to other destinations. This bottleneck will be avoided in the future by using photonic networks, in which signals are routed optically toward their destinations without requiring conversion to the electronic domain at the intermediate nodes. One approach to photonic networking, which currently is receiving the attention of many researchers, is to use the wavelength of a signal to determine its destination address and to route the signals by using wavelength-selective elements at the network nodes. In practice it is found that the restricted number of discrete wavelength channels that can be accommodated limits the extent of such a network unless wavelength conversion is used at the nodes. This has driven a large research activity in wavelength conversion techniques (*10*). An alternative approach is to use optical packet networks (*11, 12*), in which the destination address is coded within each data packet (*12*), which has the advantage of using logical addressing, as in electronic data networks, to give a near infinite address space. In the future, digital processing techniques could be used not only for wavelength conversion, 3R regeneration, and destination-address recognition but also to enable routing, error detection, coding, and other low-level signal-processing functions. These functions could be performed on the fly at ultrafast speed in the optical domain, thus alleviating bottlenecks at electronic packet switches and routers. In the future this approach could allow more efficient use of resources for ultra-high-capacity data networking by allowing statistical multiplexing of traffic and rapid network adaptation at the physical level.

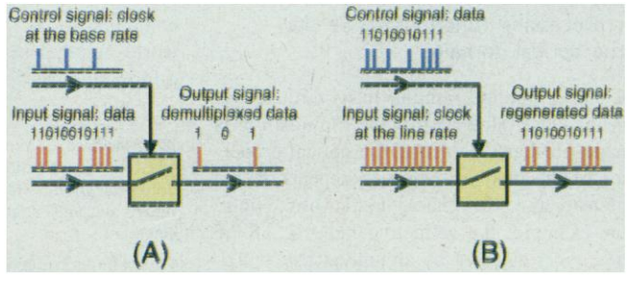

Fig. 1. Nonlinear optical gate used as a high-speed digital demultiplexer (**A**) and as a regenerator (**B**). Arrival of an optical control pulse causes the gate to transmit a single optical input bit. For the demultiplexer, the control signal is a regular periodic pulse train (clock) at the bit rate of the demultiplexed channel (base rate). For the regenerator, the control signal is random binary data.

Nonlinear Optical Switch

The basic processing element needed for high-speed digital optical processing is a fast-gating device, which allows one optical signal to control a gate that switches a second optical signal (all-optical switching). The device that has proved most successful is some form of nonlinear interferometer, and the Sagnac, Mach-Zehnder, and Michelson configurations have all been used in systems experiments (*13*). The basic operation is the same for all configurations. The input signal, which is to be switched, is split between the arms of the interferometer. The interferometer is balanced so that, in the absence of a control signal, the input signal emerges from one output port. The effect of applying the control signal is to induce a differential phase shift, $\Delta\Phi$, between the two arms so that the input signal is switched over to a second output port. In the case of the Sagnac interferometer, one of the output ports also serves as the input port for the switched signal (Fig. 2A).

The first demonstrations of ultrafast processing with an optical fiber interferometer used the Sagnac configuration, best known as the nonlinear optical loop mirror (NOLM) (*14*) (Fig. 2A), in which the nonlinear element is a length of optical fiber (the offset x can be disregarded at present). The Sagnac configuration has the advantage of greater inherent stability than other fiber interferometers. The input coupler splits the input signal pulse into two counterpropagating pulses, which subsequently combine again at the coupler, each having traveled around the loop. The usual method of breaking the symmetry of the interferometer is to insert a powerful control pulse into the loop as a unidirectional beam. The nonlinear optical effect of the control pulse is to induce a refractive index change, Δn, which is experienced fully by a copropagating signal pulse but to a much lesser degree by a counterpropagating signal pulse. This refractive index change results in a differential phase shift, $\Delta\Phi$, between the counterpropagating signal pulses as they arrive back again at the input coupler, given by $\Delta\Phi = k\Delta nL$, where k is the wavevector and L is the path length over which the induced index change Δn is effective. Typically, the control pulse should induce a differential phase shift, $\Delta\Phi = \pi$ radians, to effect complete switching. Truly ultrafast processing is possible in a fiber interferometer because the physical mechanism is the intrinsic nonlinear optical refraction of the glass, whose response and relaxation times are believed to be a few femtoseconds (*3*). The main drawbacks stem from the very small optical nonlinearity of glass ($n_2 \approx 3 \times 10^{-20}$ m^2 W^{-1} for silica), and therefore a device control power-length product of typically ~1 Wkm is needed to achieve $\Delta\Phi = \pi$. In practice, fiber interferometer path lengths

of several kilometers are needed to keep the average control power to a reasonable level (<100 mW). For lengths greater than a few hundred meters, the stability of the NOLM is significantly degraded. The long path lengths make it difficult to create systems of more than one device and also introduce excessive latency for some processing applications.

Since the 1980s there has been much research on nonlinear optical materials to try to discover one having the advantages of silica (high transparency and ultrafast speed of response) but with much larger nonlinear coefficients. Stegeman and Miller (*15*) derived various figures of merit that gave a clear set of criteria that a material must satisfy to be of practical use. In essence, these criteria are that the nonlinear coefficients must be sufficiently large, and the optical attenuation sufficiently low, to allow $\Delta\Phi = \pi$ to be achieved at a practical optical power level. As well as these physical criteria, systems considerations dictated further requirements (*16*). The search for suitable materials was helped by the work of Sheik-Bahae *et al.* (*17*), who derived a unified model for the bound electronic nonlinearity of a wide range of dielectrics and semiconductors. However, the search proved frustrating. It gradually became clear that the necessary criteria for practical use of passive nonlinear optical materials are essentially incompatible.

Active Semiconductor-Based Switches

The breakthrough came about 6 years ago with the discovery that active semiconductor devices (with electrically injected free carriers) could be used to perform high-speed optical gating (*18*). At that time, it was already known that the semiconductor optical amplifier (SOA) is highly nonlinear in its optical properties. The SOA is similar to a semiconductor laser diode, except that the reflectivity of the end faces is deliberately minimized to suppress lasing. Much of the development effort on SOAs has, in fact, been directed to minimize the nonlinearity because it tended to introduce unwanted effects (such as frequency chirping and interchannel crosstalk) in optical communications systems. The interband nonlinear effect in an SOA is an example of a resonant process, which exhibits a large but relatively slowly relaxing response. If an optical beam is incident on a semiconductor in inversion (that is, having an injection current sufficiently large to produce optical gain) and with photon energy slightly larger than the band gap, it is amplified by stimulated emission. This process involves electronic transitions from the conduction to valence bands. The amplification saturates as the conduction band is depopulated (the valence band fills). Associated with this change in gain due to saturation is a concomitant refractive index change, as described by the Kramers-Kronig dispersion relations (*2*). To a good approximation, the refractive index for wavelengths near the band edge is proportional to the carrier density, and hence to the optical intensity, provided the gain is not fully depleted (*19*). If the saturating optical signal is removed, the refractive index relaxes to its equilibrium value with a time constant that, depending on the carrier lifetime, is typically 100 to 500 ps.

The refractive nonlinearity of the SOA is very large (>10^8 times larger than an equivalent length of silica fiber, for a 100-ps optical pulse). Moreover, Stegeman's criteria for the relative magnitudes of the refractive nonlinearity and optical loss of a practical switching device are automatically satisfied because the power of the control and switched signals is amplified in the device. Optical self-switching in a nonlinear Sagnac interferometer with an SOA was demonstrated (*20*), and the required pulse energy to achieve switching was small (~1 nJ in a 10-ns input pulse). However, until the early 1990s, researchers disregarded the SOA as a suitable device for processing high-speed optical data signals. The accepted wisdom at that time was that the nonlinear response must recover fully in the time period of 1 bit. For a typical carrier lifetime of 300 ps, this implied that the fastest data signal that could be processed is ~1 Gbit/s, too slow to be of practical interest because this does not compete effectively with electronic processing equipment. Then came two key developments that have changed the scene altogether.

The first key step was development of nonlinear Sagnac interferometers in which a short nonlinear element is positioned asymmetrically with respect to the center of the loop (offset x in Fig. 2A). This arrangement [using either self-switching (*21*) or controlled switching (*22, 23*)] could be used to obtain a very short switching window, shorter than the recovery time of the nonlinear refractive index. When the nonlinear element is an SOA, the asymmetric Sagnac interferometer is known by the acronym SLALOM (semiconductor laser amplifier in a loop mirror) (*22*) or TOAD (terahertz optical asymmetric demultiplexer) (*23*). When the interferometer is used to demultiplex a lower speed channel from a high-speed data signal (Fig. 1A), the control signal in Fig. 2A is a regular periodic pulse train (called the clock) at the base rate (the bit rate of the demultiplexed channel). The control signal is at a different wavelength (or polarization) from the data-modulated input pulse train and is injected into the SOA with a wavelength coupler (or polarization coupler). After passing through the SOA, the control pulse is coupled out of the loop mirror. The equilibrium balance of the interferometer is set so that, in the absence of a control pulse, no input signal appears at the output port. When a data pulse arrives, it is split into clockwise (cw) and counterclockwise (ccw) traveling components by the input coupler. The fact that the SOA is positioned asymmetrically within the loop means that the cw component arrives at the SOA before the ccw component. Whether the loop is operated in the SLALOM (*22*) or TOAD (*23*) mode depends on the relative timing between the control and input data pulses. In SLALOM operation the control pulse arrives at the SOA before either of the counterpropagating input data pulses. In TOAD operation, the control pulse is timed to arrive after the cw data pulse has passed through the SOA but before the ccw pulse has arrived (Fig. 3). The control pulse rapidly sweeps out some of the gain in the SOA, creating a refractive index change that corresponds to the differential phase shift $\Delta\Phi \approx \pi$ experienced by the cw data pulse. Upon arrival back at the coupler, the phase difference between the cw and ccw pulse means that the recombined data pulse exits from the output port. Subsequent data pulses (in the absence of a clock pulse) experience a gain and refractive index that is slowly recovering; hence the cw and ccw pulses have only a very small phase difference and so after recombining do not appear at the output port. The important aspect of the asymmetric interferometer is that the offset distance x of the SOA from the loop center, rather than the relaxation time of the nonlinear effect, determines the time width of the switching window. Therefore, by suitable choice of window, the effect of a single clock pulse is to switch a single input data bit to the

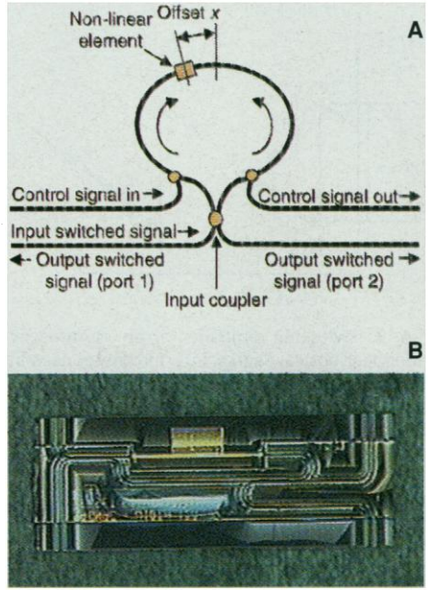

Fig. 2. (**A**) Optical circuit diagram of a nonlinear Sagnac interferometer configured as an optical gate. (**B**) A realization of this circuit on a single 1 × 2 mm indium phosphide semiconductor chip, photographed before packaging.

output port. It was demonstrated that a window width of ≤10 ps could be created, allowing a very high speed pulse train (~50 GHz) to be demultiplexed down to a base rate of ~1 GHz (*24*). However, at first it was believed that the base rate would remain limited by the time for the induced gain and refractive index changes in the SOA to decay fully.

The second key development was the discovery that the asymmetric Sagnac interferometer could be used effectively as a demultiplexer at a base rate of 10 GHz (*18*). This was clearly much faster than the natural recovery rate of ~1 GHz. Since then, several other groups have also demonstrated demultiplexing to a 10-Gbit/s base rate (*25*), with initial data rates as high as 160 Gbit/s (*26*). Manning *et al.* (*27*) explained these results by considering the SOA carrier dynamics in detail. Two important factors were realized. First, the carrier density change required for a differential phase shift, $\Delta\Phi = \pi$, is small compared with the inversion normally available. For a 500-μm-long SOA, and a wavelength of 1.5 μm, $\Delta\Phi = \pi$ corresponds to a change in the refractive index of 10^{-3}. Therefore, given that the rate of change of refractive index with electron-hole pair density is -2×10^{-20}, a carrier population change of only $\sim 10^{17}$ cm^{-3} is needed, compared with a typical inversion of $\sim 10^{18}$ cm^{-3}. Hence a differential phase shift of magnitude several π can be achieved by saturating the SOA gain. Second, the rate at which carriers are replenished by the typical SOA injection current (a few tens of milliamperes) is surprisingly high. Assuming the injection current maintains a typical equilibrium carrier density of 2×10^{18} cm^{-3} and the carrier lifetime is ~500 ps, then the rate of carrier injection via the current is $\sim 4 \times 10^{15}$ cm^{-3} ps^{-1}. Remarkably, this implies replenishment of 10^{17} cm^{-3} carriers in only ~25 ps. It follows then that the injection current is sufficient to cause a phase recovery of π in a very short time. This is the rate of recovery when the gain is strongly saturated by optical pumping, so the carrier density is far from its equilibrium value. Combining these two factors—the relatively small carrier density change needed and the high rate of electrical carrier injection—means that an incremental phase change of π can decay in a time that is a small fraction of the carrier lifetime. Detailed modeling has shown that this successfully explains how the nonlinear interferometer is capable of fast switching (Fig. 3). Experimental measurements under conditions of higher current densities, and hence shorter carrier lifetimes, showed that the injection current can restore a differential phase shift of π radians in as little time as ~10 ps (*28*), implying that operation at demultiplexer base rates as high as 100 Gbit/s should be possible. Experimental support for this prediction was obtained recently when it was shown that the underlying physical mechanism, cross-gain modulation in the SOA, is capable of operation at 100 GHz (*29, 30*). The required energy of the control pulse is found to be as low as ~100 to 200 fJ (*26, 31*). The predicted average power of the control signal for a demultiplexer at a 100-Gbit/s base rate is therefore ~10 to 20 mW, well within the range of practical devices.

In practical terms, another important recent advance has been the development of optical interferometric switches comprising SOAs, waveguides, and optical couplers fully integrated on a single semiconductor chip (Fig. 2B). Several types of interferometer, such as the Sagnac (*31*), Michelson (*32*), and Mach-Zehnder (*25*), have been fabricated in this way and used successfully in optical systems experiments (*33*).

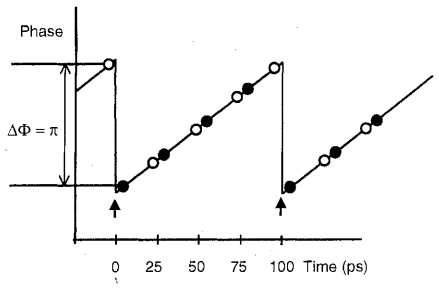

Fig. 3. Switching dynamics of an asymmetric nonlinear optical Sagnac interferometer used in the TOAD configuration. Results of a numerical simulation show the phase change induced by the control signal and the resulting differential phase for the counterpropagating components of the input data signal. Arrival times for the various optical signals at the SOA are indicated by different symbols: ↑, control pulse; ○, clockwise input signal; ●, counterclockwise input signal. Difference in arrival times or counterpropagating input signals is determined by offset *x* shown in Fig. 2. The control signal here is assumed to be a regular periodic pulse train (clock) at a base rate of 10 GHz, and the counterpropagating pairs of data bits occur at 40 Gbit/s (25-ps bit period).

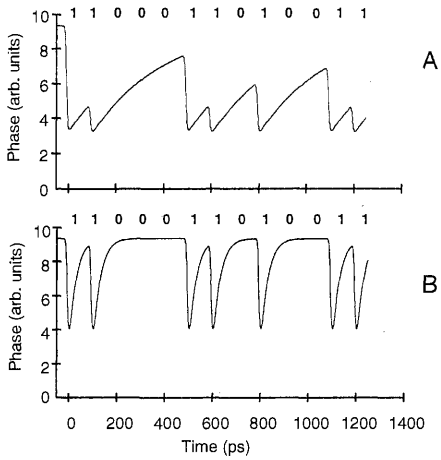

Fig. 4. Data pattern dependency of the induced phase of the SOA when the control signal is a random binary data sequence (1100011 010011) at the rate 10 Gbit/s. Curves are results of numerical simulations assuming a carrier lifetime of 300 ps (**A**) and 30 ps (**B**) and show effective suppression of pattern effects for the shorter carrier lifetime.

Optical Digital Regenerator

The various developments up to the mid-1990s showed that compact semiconductor-based nonlinear interferometers are useful as demultiplexing gates for very high speed data signals. However, difficulties were encountered at first when these gates were tested for use in another very important application: high-speed digital optical 3R regeneration. The method for optical regeneration of a return-to-zero digital data stream (*8, 9*) (Fig. 1B) is that the incoming data bits from a distant source are used to modulate a continuous train of high-quality pulses produced by a synchronous local source, thus regenerating the original data. Each data bit "1" in the incoming data causes the gate to switch to transmission mode for a fixed time (the gate window), allowing a single pulse from the local source to pass through. In this way, the regenerated bits have essentially the same pulse shape, spectral quality, amplitude, and timing stability as the local source. Moreover, the regenerator can tolerate a degree of jitter in the arrival time of the data bits, determined by the gate window width. All-optical 3R regeneration was successfully demonstrated with a fiber NOLM as the switching gate (*8*). However, when the semiconductor-based nonlinear interferometer was used as the gate, it proved difficult at first to obtain error-free operation.

The reason for this difficulty again can be understood from the carrier dynamics in the SOA. The crucial point is that when the nonlinear interferometer is used as a demultiplexer, the control signal is a regular train of clock pulses. In that case the induced phase changes are regular and periodic (Fig. 3). In contrast, the phase shifts are entirely irregular when the control signal consists of random binary data (as in the regenerator). Numerical calculation of the variation in phase when a random data sequence travels through an SOA under typical conditions (Fig. 4A) shows that large-phase excursions occur whenever several data bits "0" appear consecutively, because there is then sufficient time for the gain to recover substantially. A "1" bit following a sequence of zeros will experience a larger gain than the previous "1," causing a larger phase change. A way of overcoming this data-pattern dependency to some degree is to enhance the recovery rate so that substantial gain recovery occurs in the

time of one bit period. This can be done by increasing the injection current and also by deliberately reducing the carrier lifetime by stimulated emission at the wavelength of the control pulse or another optical signal (*27*). By reducing the carrier lifetime to ~30 ps (Fig. 4B), any control data bit "1" will cause essentially the same phase change in the SOA. However, the effect of reducing the carrier lifetime is also to reduce the available phase change. Therefore, some compromise is necessary between the levels of injection current and optical input powers. It is also found beneficial to use a relatively long SOA (up to 2-mm active region) and to optimize the design of the multiquantum well gain region to maximize the optical nonlinearity (*34*).

Successful operation of nonlinear semiconductor interferometers with very high speed control signals consisting of random binary data has been achieved recently. Wavelength conversion at 40 Gbit/s (*35*) and 100 Gbit/s (*36*) and 3R regeneration at 20 Gbit/s (*37*) and 40 Gbit/s (*38*) have been reported. In the case of the wavelength convertors, one of the inputs is a continuous-wave signal, which has the effect of reducing the carrier lifetime by stimulated emission, as explained above. For the regenerators, good operation is found by using a relatively high-power clock input (typically only 3 dB lower than the control signal power), and this again produces the desired shortening of the carrier lifetime. The good cascadability of the devices was demonstrated by incorporating a 40-Gbit/s 3R regenerator in a recirculating loop (*39*). It was shown that adequate switching windows are attainable to allow 100-Gbit/s digital optical logic (*29*). Recently Kelly *et al.* (*30*) confirmed error-free operation at these high bit rates with demonstration of 80-Gbit/s optical regeneration using a nonlinear Mach-Zehnder interferometer containing an SOA, with a control pulse energy of ~200 fJ. Figure 5 is an "eye" diagram (a probability histogram of the amplitude of a random data signal plotted as a function of time) of the 80-Gbit/s signal before and after regeneration. Measurements of the bit-error rate at the output of the regenerator after demultiplexing to a 10-Gbit/s base rate showed a bit-error probability of $<10^{-9}$ and a power penalty of 2.7 dB, for a pseudorandom binary data sequence with pattern length $2^{31} - 1$.

Ultimate Limits to Speed

The highest speed of operation of a semiconductor nonlinear interferometer is obtained by judicious choice of the injection current, optical powers, and other device parameters. The ultimate limiting speed is the time to establish an equilibrium Fermi-Dirac distribution of the carrier population, which is believed to be ~5 ps (*40*). This means that switching rates as high as 200 GHz are theoretically possible. The 80-Gbit/s regenerator recently demonstrated (*30*) might be approaching the fastest speed that can be achieved in practice with a single gate controlled by a random data signal, the main limitation being data-pattern effects. However, a gate used as a demultiplexer is relatively free from pattern effects and can be operated at higher data rates. This suggests a simple way of extending the maximum speed of an optical regenerator system (Fig. 6). For example, a combination of two 160-Gbit/s demultiplexing gates (*26*) with two 80-Gbit/s regenerative gates (*30*) could provide a digital regenerator operating at 160 Gbit/s.

All the semiconductor devices we have described until now rely on optical nonlinearity (either gain/loss or refractive) caused by the real transfer of carriers between conduction and valence bands in the SOA—in other words the real exchange of energy between the optical fields and the material. Yet higher speed of operation can be obtained by nonlinear processes that involve intraband transitions. These consist of a virtual exchange of energy between the field and the medium and allow ultrafast parametric effects such as four-wave mixing (*2*). The time scale of these virtual processes in SOAs is known to be in the subpicosecond regime (*40*), and therefore operation at speeds up to 1 Tbit/s is theoretically possible. Typically, four-wave mixing involves injecting two or more optical signals into the SOA, resulting in generation of optical sidebands. These sidebands may be isolated by filtering and then used for applications such as optical time-domain sampling (*41*), wavelength conversion (*42*), or dispersion compensation (*43*), or to provide an optical AND logic gate (*44*). For wavelength conversion or dispersion compensation the data signal is mixed with a continuous-wave pump wave. For the AND gate or optical time-domain sampling, two pulsed signals are mixed together in the presence of a pump wave to produce a fourth output signal; this output is present only when the two input pulsed signals are coincident in time. It has been demonstrated recently that these processing devices can operate without errors at 100 Gbit/s (*41, 45*), and devices at that speed have been used to recognize the destination addresses of optical packets (*46*), achieve bit-level synchronization (*47*), and perform clock recovery (*48*).

First proof-of-principle demonstrations of a variety of digital optical processing func-

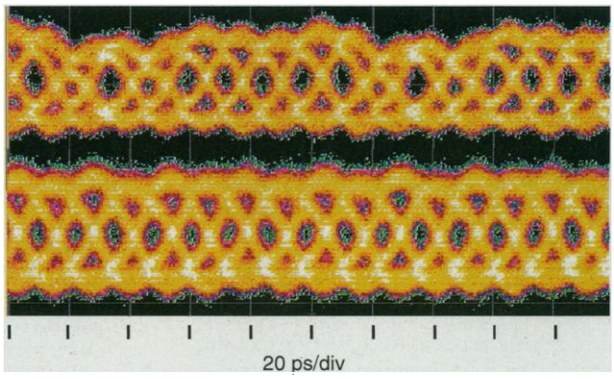

Fig. 5. Measured color-graded "eye" diagram (probability histogram of signal amplitude versus time) of an 80-Gbit/s pseudorandom binary data signal (12.5-ps bit period), shown before (upper) and after (lower) optical regeneration in a nonlinear Sagnac interferometer containing a semiconductor optical amplifier. Diagrams were recorded with a photodetector with 30-GHz bandwidth and displayed on a 50-GHz sampling oscilloscope. Although these high-speed data signals are poorly resolved with this electronic display system, considerable nonuniformity between the eight 10-Gbit/s base channels is clearly visible. Also visible is equalization of the channel amplitudes at the output of the regenerator.

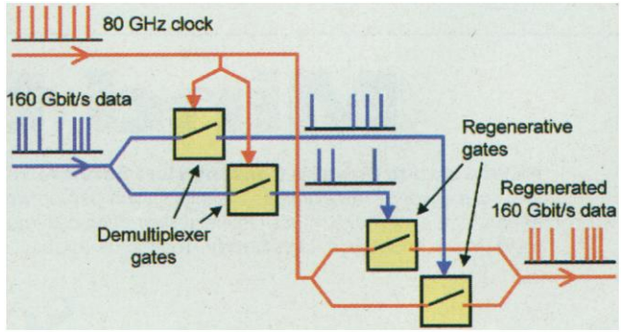

Fig. 6. Concept for an ultra-high-speed digital optical regenerator system consisting of four nonlinear optical gates. Two gates are used as demultiplexers to produce two orthogonal data channels at lower speed, and two gates are used to regenerate these data signals before bit interleaving to produce the regenerated output at the full line rate. In principle, the regenerator could be extended to yet higher bit rates by increasing the number of gates.

tions have been made recently by combining two or three interferometric gates in various simple optical circuits (albeit so far at the relatively low speed of ~1 Gbit/s). These have included a shift register with inverter, a regenerative memory with logic level restoration, an optical memory with read/write ability, a binary half-adder, a pseudorandom number generator, and a parity checker (*49*).

Prospects

Until now, the main challenge for researchers has been to determine what is physically possible and practical for high-speed digital optical logic gates. The field has been largely transformed by the advent of semiconductor devices capable of operation at 100 Gbit/s and potentially higher speeds. Work will continue apace to develop and refine new devices and circuits and to increase the degree of component and device integration. Techniques such as wavelength conversion and optical 3R regeneration are likely to reach commercial application within 1 to 3 years. On a similar time scale, the first prototype devices capable of regenerating data in multiple wavelength channels simultaneously probably will emerge in research laboratories. Demultiplexing gates and elementary logic will be used to enable recognition of flags, symbols, and words at the full-line transmission rate. Later, digital optical devices could allow higher-level processing on the fly in the optical domain, such as error detection, header translation, coding, and encryption.

The most interesting and difficult challenge facing researchers will be to determine not so much whether and how high-speed digital optical devices and processing systems can be made but rather how they can best be applied to useful effect in communications networks. A fundamental difference between electronics and photonics is that optical signals necessarily consist of traveling waves. The most important manifestation of this difference in information systems is the lack of an optical equivalent of electronic static random-access memory. The photonic systems designer is therefore forced to invent new network architectures and protocols rather than simply imitate the designs developed by electronics engineers. For example, new strategies are needed to resolve contention (which arises when two data packets are routed toward the same pipe simultaneously) in a way that overcomes the lack of static optical memory.

It is unlikely that photonics will compete with the dense integration and rich functionality of electronics, at least for very many years to come. Nevertheless, the digital optical devices being developed in research laboratories today can already offer advantages in terms of speed and compatibility with optical transmission systems. We envisage that within a few years modest numbers of high-speed nonlinear optical devices, processing optical signals on the fly, will be used in tandem with electronics to increase greatly the capacity and throughput of communications networks.

References

1. N. Bloembergen, *Nonlinear Optics* (World Scientific, Singapore, ed. 4, 1996).
2. P. N. Butcher and D. Cotter, *The Elements of Nonlinear Optics* (Cambridge Univ. Press, Cambridge, 1990).
3. G. P. Agrawal, *Nonlinear Fiber Optics* (Academic Press, San Diego, CA, ed. 2, 1995); R. H. Stolen, *Proc. IEEE* **68**, 1232 (1980); D. Marcuse, in *Optical Fiber Telecommunications II*, S. E. Miller and I. P. Kaminow, Eds. (Academic Press, Boston, 1988).
4. A. R. Chraplyvy, *J. Lightwave Technol.* **8**, 1548 (1990); F. Forghieri *et al.*, in *Optical Fiber Telecommunications IIIA*, T. L. Koch and I. P. Kaminow, Eds. (Academic Press, New York, 1997).
5. H. Onaka *et al.*, *Proc. Optical Fiber Conf.*, San Jose, CA, paper PD19 (1996); A. R. Chraplyvy *et al.*, *IEEE Photon. Technol. Lett.* **8**, 1264 (1996); T. Morioka *et al.*, *Electron. Lett.* **32**, 906 (1996); *Y. Yano et al.*, *Proc. ECOC'96* (European Conf. Opt. Commun.), paper ThB.3.1; S. Kawanishi *et al.*, *Electron. Lett.* **33**, 1716 (1997); A. R. Chraplyvy *et al.*, *IEEE J. Quantum Electron.* **34**, 2103 (1998).
6. M. Nakazawa *et al.*, *Electron. Lett.* **34**, 907 (1998); T. Yamamoto *et al.*, *Electron. Lett.* **34**, 1013 (1998).
7. K. J. Blow *et al.*, *Electron. Lett.* **26**, 962 (1990).
8. M. Jinno and M. Abe, *Electron. Lett.* **28**, 1350 (1992); J. K. Lucek and K. Smith, *Opt. Lett.* **18**, 1226 (1993).
9. D. Cotter and A. D Ellis, *J. Lightwave Technol.* **16**, 2068 (1998).
10. S. Diez *et al.*, *IEEE J. Sel. Topics Quantum Electron.* **3**, 1131 (1997).
11. D. Cotter *et al.*, in *Photonic Networks*, G. Prati, Ed. (Springer, London, 1997); D. K. Hunter *et al.*, *J. Lightwave Technol.* **16**, 2081 (1998); C. Guillemot, *J. Lightwave Technol.* **16**, 2117 (1998); A. Carena *et al.*, *J. Lightwave Technol.* **16**, 2135 (1998); V. W. S. Chan *et al.*, *J. Lightwave Technol.* **16**, 2146 (1998); P. Toliver *et al.*, *J. Lightwave Technol.* **16**, 2169 (1998), K. H. Ahn *et al.*, *IEEE Photon. Technol. Lett.* **11**, 140 (1999); D. K. Hunter *et al.*, *IEEE Comm. Mag.* **37**, 120 (1999).
12. D. J. Blumenthal *et al.*, *Proc. IEEE* **82**, 1650 (1994).
13. K. I. Kang *et al.*, *Int. J. High Speed Electron. Sys.* **7**, 125 (1996).
14. N. J. Doran and D. Wood, *Opt. Lett.* **13**, 56 (1988).
15. G. I. Stegeman and A. Miller, in *Photonics in Switching I*, J. E. Midwinter, Ed. (Academic Press, London, 1993).
16. D. Cotter, *Nonlinear Optics* **13**, 185 (1995).
17. M. Sheik-Bahae *et al.*, *IEEE J. Quant. Electron.* **27**, 1296 (1991).
18. A. D. Ellis and D. M. Spirit, *Electron. Lett.* **29**, 2115 (1993).
19. M. J. Adams *et al.*, *Opt. Quantum Electron.* **27**, 1 (1995).
20. A. W. O'Neill and R. P. Webb, *Electron. Lett.* **26**, 2008 (1990).
21. D. Cotter *et al.*, U.S. patent 4,973,122 (1990).
22. M. Eiselt *et al.*, *Electron. Lett.* **28**, 1505 (1992).
23. J. P. Sokoloff *et al.*, *IEEE Photon. Technol. Lett.* **5**, 787 (1993).
24. J. P. Sokoloff *et al.*, *IEEE Photon. Technol. Lett.* **6**, 98 (1994).
25. E. Jahn *et al.*, *IEEE Photon. Technol. Lett.* **31**, 1857 (1995).
26. K. Suzuki *et al.*, *IEEE Photon. Technol. Lett.* **30**, 1501 (1994).
27. R. J. Manning *et al.*, *J. Opt. Soc. Am. B* **14**, 3204 (1997).
28. R. J. Manning and G. Sherlock, *J. Opt. Soc. Am. B.* **31**, 307 (1995).
29. K. L. Hall and K. A. Rauschenbach, *Opt. Lett.* **23**, 1271 (1998).
30. A. E. Kelly *et al.*, *Electron. Lett.* **35**, 1477 (1999).
31. E. Jahn *et al.*, *Electron. Lett.* **32**, 782 (1996).
32. B. Mikkelsen *et al.*, *Proc. ECOC'94* (European Conf. Opt. Commun.), **4**, 67 (1994).
33. E. Jahn *et al.*, *Electron. Lett.* **32**, 216 (1996); S. L. Danielsen *et al.*, *IEEE Photon. Technol. Lett.* **8**, 434 (1996).
34. A. E. Kelly *et al.*, *Electron. Lett.* **33**, 2123 (1997).
35. B. Mikkelsen *et al.*, *Electron. Lett.* **33**, 133 (1997).
36. A. D. Ellis *et al.*, *Electron. Lett.* **34**, 1958 (1998).
37. L. Billes *et al.*, in *Proc. IOOC-ECOC'97* (European Conf. Opt. Commun.) (IEE Conf. Publ. no. 448), **2**, 269 (1997).
38. I. D. Phillips *et al.*, *Electron. Lett.* **34**, 2340 (1998).
39. H. J. Thiele *et al.*, *Electron. Lett.* **35**, 230 (1999).
40. K. L. Hall *et al.*, *Opt. Commun.* **111**, 589 (1994).
41. K. Uchiyama *et al.*, *IEEE Photon. Technol. Lett.* **10**, 890 (1998).
42. M. C. Tatham *et al.*, *IEEE Photon. Technol. Lett.* **5**, 1303 (1993).
43. D. D. Marcenac *et al.*, *Electron. Lett.* **33**, 879 (1997).
44. D. Nesset *et al.*, *Electron. Lett.* **30**, 1938 (1994); D. Nesset *et al.*, *Electron. Lett.* **31**, 896 (1995).
45. A. E. Kelly *et al.*, *Electron. Lett.* **34**, 1955 (1998).
46. D. Cotter *et al.*, *Electron. Lett.* **31**, 1475 (1995).
47. M. Shabeer *et al.*, *Electron. Lett.* **31**, 1476 (1995).
48. O. Kamatani and S. Kawanishi, *J. Lightwave Technol.* **14**, 1757 (1996).
49. A. J. Poustie *et al.*, *Opt. Commun.* **159**, 208 (1999), and references therein; A. J. Poustie *et al.*, *Opt. Commun.* **162**, 37 (1999).